Published in final edited form as:
Clin Cancer Res. 2012 October 15; 18(20): 5788–5795. doi:10.1158/1078-0432.CCR-12-1967.

Ontogeny and sorafenib metabolism

Eric I. Zimmerman[1], **Justin L. Roberts**[1], **Lie Li**[1], **David Finkelstein**[2], **Alice Gibson**[1], **Amarjit S. Chaudhry**[1], **Erin G. Schuetz**[1], **Jeffrey E. Rubnitz**[3], **Hiroto Inaba**[3], and **Sharyn D. Baker**[1]

[1]Department of Pharmaceutical Sciences, St. Jude Children's Research Hospital, Memphis, TN USA

[2]Department of Information Sciences, St. Jude Children's Research Hospital, Memphis, TN USA

[3]Department of Oncology, St. Jude Children's Research Hospital, Memphis, TN USA

Abstract

Purpose—To investigate the role of ontogeny in sorafenib metabolism to the equipotent active metabolite sorafenib N-oxide.

Experimental Design—Steady-state pharmacokinetic studies of sorafenib and metabolites were performed in thirty children and young adults (17 males; median age, 9.5 years) receiving sorafenib 150 mg/m^2 or 200 mg/m^2 twice daily. Sorafenib metabolism was evaluated *in vitro* at 10 μM using a panel of purified human cytochrome P450 (CYP) enzymes. Sorafenib metabolism and CYP3A4 expression was evaluated in 52 human liver samples from donors ≤ 20 years old. The drug-drug interaction potential between sorafenib and azole antifungal agents was evaluated *in vitro* and *in vivo*.

Results—No age-related differences in sorafenib apparent oral clearance were observed. Mean sorafenib N-oxide metabolite ratio was 0.27±0.14. In children ≤ 10 years of age, boys had approximately 2-fold higher N-oxide ratios than girls (0.40±0.15 *versus* 0.22±0.12, $P = 0.026$). Of the CYPs evaluated, sorafenib was exclusively metabolized to sorafenib N-oxide by CYP3A4. A trend for increased N-oxide formation in boys was observed in liver samples, which correlated with CYP3A4 mRNA expression. Posaconazole and voriconazole potently inhibited sorafenib N-oxide formation *in vitro*, and reduced sorafenib N-oxide formation in 3 children given sorafenib concurrent with azoles.

Conclusion—We have identified several factors affecting inter-patient variability in sorafenib metabolism to the active N-oxide metabolite including age, sex, and concurrent treatment with azole antifungals. This knowledge may provide important considerations for the clinical use of sorafenib in children and possibly other kinase inhibitors undergoing CYP3A4-mediated metabolism.

Keywords

sorafenib; ontogeny; metabolism; CYP3A4; UGT1A9; drug-drug interaction

Correspondence: Sharyn D. Baker, PharmD, PhD, Department of Pharmaceutical Sciences, St. Jude Children's Research Hospital, 262 Danny Thomas Place, Memphis, TN 38105, CCC Room I5306, Memphis TN, USA. Phone: (901) 595-3089, Fax: (901) 595-3125, sharyn.baker@stjude.org.

Conflicts of Interest: Dr. Inaba receives research funding from Bayer Pharmaceutical. All other authors declare no potential conflict of interest.

Introduction

Sorafenib is a multi-kinase inhibitor with activity against c-RAF, B-RAF, c-KIT, FLT3, platelet derived growth factor receptor (PDGFR) α and β, vascular endothelial growth factor receptor (VEGFR) 1, 2, and 3, and multiple other kinases (1). It is approved for the treatment of advanced renal cell carcinoma and hepatocellular carcinoma and is being evaluated in acute myeloid leukemia (AML) (2). Sorafenib is metabolized by UDP-glucuronosyltransferase 1A9 (UGT1A9) to sorafenib glucuronide and by CYP3A4 to the active metabolite sorafenib N-oxide (3, 4). Sorafenib N-oxide has been reported to represent approximately 10% of circulating sorafenib concentrations in healthy subjects and cancer patients (3, 5). Recently, we reported a substantially higher rate of conversion of sorafenib to sorafenib N-oxide (33%) in twelve children with relapsed/refractory AML compared to adults with AML (<10%) (6, 7). Despite a higher rate of metabolism to sorafenib N-oxide, sorafenib exposure was not reduced in children compared to values observed in adults at equivalent doses. We demonstrated that sorafenib N-oxide has similar kinase inhibitory activity as sorafenib in a 442-kinase panel and exhibited cytotoxic activity in AML cell lines, suggesting that combined exposure to both sorafenib and sorafenib N-oxide may contribute to overall anti-leukemic activity, especially in children (6).

To elucidate mechanisms involved in differential sorafenib metabolism between children and adults, we characterized sorafenib metabolism to sorafenib N-oxide and sorafenib glucuronide in a cohort of thirty children with AML. As a complement, we also evaluated sorafenib metabolism and CYP3A4 and UGT1A9 gene expression in 52 human liver samples from patients of ages 1 to 20 years. We evaluated sorafenib metabolism using a panel of purified human UGT and CYP enzymes, and determined the drug-drug interaction potential between sorafenib and azole antifungal agents *in vitro* and *in vivo*.

Patients and Methods

Children and young adults with FLT3-ITD-positive AML were enrolled in the frontline trial AML08 (clinical trials.gov identifier NCT00703820) and treated with sorafenib 200 mg/m^2 twice daily after Induction II therapy with cytarabine, daunorubicin, and etoposide. Children and young adults with relapsed or refractory AML were enrolled to the trial RELHEM (clinical trials.gov identifier NCT00908167) and treated with sorafenib 150 mg/m^2 or 200 mg/m^2 twice daily as described previously (6). Concomitant treatment with drugs known to inhibit or induce CYP3A4, including azole antifungals, was excluded unless medically indicated. Two patients with FLT3-ITD-positive AML who were initially enrolled on RELHEM or AML08 were further treated long-term with single-agent sorafenib concurrently with an azole antifungal. All protocols and treatments were approved by the institutional review boards and informed consent was obtained from all patients or their legal guardians.

Pharmacokinetic Studies

Peripheral blood was collected on days 7 (RELHEM trial) or day 8 (AML08 trial) before and 2, 4.5, and 7.5 h after sorafenib administration. Samples were centrifuged for 10 min at 3000 g and plasma was stored at −80°C until analysis. A blood sample was obtained pre-treatment (trough) and throughout therapy from patients receiving sorafenib long-term with concurrent azole antifungals. The concentration of sorafenib, sorafenib N-oxide, and sorafenib glucuronide was measured using a validated HPLC-based method with tandem mass spectrometric detection as described in the Supplemental Materials. Average steady-state plasma concentration (Css,ave) for each analyte was estimated 2 ways: 1) as the mean concentration of the 4 samples collected on the specified day, since the concentration-time profiles showed minimal fluctuations from maximum to minimum during the sampling

interval; and 2) as AUC over the dosing interval of 12 h (AUC0-12h) divided by the dosing interval. For the latter, AUC0-12h was calculated using the pre-dose concentration as the 12 hour concentration since troughs should be constant at steady state. All trough concentrations were obtained within 30 minutes prior to administration of the dose. Values for Css,ave calculated by both methods were within 4.0%, 0.7% and 3.5% of each other for sorafenib, sorafenib N-oxide, and sorafenib glucuronide, respectively. Css,ave values reported in this study were estimated using the first method described above. Steady-state sorafenib apparent oral clearance was estimated as sorafenib dosing rate (dose/dosing interval of 12 h) divided by Css,ave and was normalized to body surface area. Metabolite ratios were determined as the metabolite Css,ave divided by sorafenib Css,ave.

In vitro studies

Sorafenib metabolism to sorafenib N-oxide by human CYP1A1, CYP1A2, CYP3A4, CYP3A5, CYP2C8, CYP2C9, CYP2C19, and CYP2D6 was determined. Sorafenib metabolism to sorafenib glucuronide by human UGT1A1, UGT1A3, UGT1A4, UGT1A6, UGT1A7, UGT1A8, UGT1A9, UGT1A10, UGT2B4, UGT2B7 and UGT2B15 was also assessed. The ability of azole antifungals to inhibit sorafenib CYP3A4- and UGT1A9-mediated metabolism was studied. Sorafenib CYP3A- and UGT-mediated metabolism and CYP3A4 and UGT1A9 gene expression were determined in 52 human liver samples from donors 1 to 20 years old. Liver tissue was processed through the Liver Resource at St. Jude Children's Research Hospital and was provided by the Liver Tissue Procurement and Distribution System (NIH Contract #N01-DK-9-2310) and by the Cooperative Human Tissue Network. Detailed descriptions of the *in vitro* experiments are found in the Supplemental Materials.

Statistical Considerations

Comparisons of metabolite ratios or metabolite formation velocity between males and females within different age groups (≤ 10 years and > 10 to ≤ 20 years) were performed using the nonparametric Wilcoxon rank-sum test. The age of 10 years was selected as an arbitrary cutoff for analysis to compare sorafenib metabolism between younger and older children. Data for gene expression in human liver samples were $\log_2$ transformed prior to comparisons in accordance with gene expression literature (8). Linear regression analysis was conducted to assess the correlation between sorafenib metabolic pathways (sorafenib N-oxide metabolic ratio *versus* sorafenib glucuronide metabolite ratio); and CYP3A4 or UGT1A9 mRNA expression *versus* metabolite velocity. Inter-patient variability was estimated as the coefficient of variation, calculated as the standard deviation divided by the mean and expressed as a percentage (CV%). Statistical significance was assigned if $P < 0.05$.

Results

Sorafenib Pharmacokinetics and Metabolism

Pharmacokinetic studies were conducted in 30 children and young adults (17 males, 13 females) with AML from November 2008 to January 2012. The median age was 9.5 years (range, 1 to 19 years). Six patients were treated with 150 mg/m^2 sorafenib and 24 patients with 200 mg/m^2. Individual patient demographics and steady-state pharmacokinetic parameters for sorafenib and metabolites are summarized in Supplemental Table 1. Mean steady-state sorafenib and metabolite concentration-time profiles at 150 mg/m^2 and 200 mg/m^2 are illustrated in Figure 1. Mean sorafenib steady-state concentration was higher at 150 mg/m^2 than at 200 mg/m^2 (7.1 versus 5.1 mg/L), which is likely due to extensive inter-subject pharmacokinetic variability of sorafenib and the smaller number of children treated at the lower dose level (6 versus 24). Mean±standard deviation steady-state sorafenib

apparent oral clearance (CL/F) was 64±37 mL/min/m^2 (CV%, 58%). No age-related differences in (CL/F) were observed, and mean CL/F was similar among males and females (males, 67±43 *versus* females, 60±28 mL/min/m^2; P=0.983) (Figure 2).

Mean sorafenib N-oxide metabolite ratio was 0.27±0.14. No sex-related differences in N-oxide metabolite ratio was observed between males and females (males, 0.26±0.15 *versus* females, 0.22±0.10; P=0.402) (Supplemental Figure 1A). Inspection of sorafenib N-oxide metabolite ratios as a function of age and sex uncovered a trend for higher sorafenib N-oxide conversion in boys than girls ≤ 10 years old, which appeared to peak in boys between approximately 6 to 10 years of age (Figure 3A). Boys had approximately 2-fold higher ratios than girls (males, 0.40±0.15 *versus* females, 0.22±0.12; P=0.026); metabolite ratios were similar among males and females older than 10 years (0.18±0.021 *versus* 0.23±0.12, respectively; P=0.061) (Figure 3B). Sorafenib N-oxide metabolite ratios were more variable in both boys and girls ≤ 10 years (CV%, 39% and 59%, respectively) compared to those greater than 10 years of age (CV%, 11% and 20%, respectively).

Mean sorafenib glucuronide metabolite ratio was 0.30±0.19, which did not vary significantly between males and females overall (P=0.438) (Supplemental Figure 1B) or in either of the two age groups (P≥0.370) (Figures 3C and 3D). Sorafenib glucuronide metabolite ratios were more variable in boys and girls in the younger age group (CV%, 71% and 70%, respectively) compared to children older than 10 years (CV%, 42% and 28%, respectively).

Sorafenib CYP- and UGT-mediated Metabolism in vitro

To comprehensively determine the enzymes responsible for sorafenib metabolism, we assessed sorafenib metabolism *in vitro* using a panel of purified human CYP and UGT enzymes. Our results demonstrated that CYP3A4 is the predominant isozyme responsible for sorafenib oxidation and UGT1A9 is primarily responsible for sorafenib glucuronidation (Supplemental Figure 2). The apparent Km was 12.1±0.71 μM for CYP3A4-mediated oxidation and 3.6±0.22 μM for UGT1A9-mediated glucuronidation.

Azole antifungal agents, including ketoconazole, voriconazole, and posaconazole, inhibit CYP3A4 activity, and ketoconazole has also been shown to inhibit UGT1A9 (9, 23). Because cancer patients are commonly treated with azoles for the prevention or treatment of invasive fungal infections, we compared the inhibitory effects of azoles on sorafenib metabolism. Azole antifungals inhibited CYP3A4-mediated sorafenib N-oxide formation with apparent Ki values of 0.16±0.09 μM, 0.38±0.09 μM, and 35.7±10.7 μM for ketoconazole, posaconazole, and voriconazole, respectively (Supplemental Figure 3). Ketoconazole inhibited sorafenib glucuronidation by UGT1A9 with an apparent Ki of 2.2 μM (Supplemental Figure 4).

Effect of Treatment with Azole Antifungals on Sorafenib N-oxide Production

One 6-year-old girl enrolled on the RELHEM protocol was receiving antifungal prophylaxis with posaconazole 140 mg every 6 hours. This patient had the lowest sorafenib N-oxide metabolite ratio in the entire population (0.05) (Supplemental Table 1). No other patients were documented to have received treatment with azoles or other strong CYP3A4 inhibitors during the sorafenib pharmacokinetic study period. However, we assessed the effect of voriconazole on sorafenib metabolism in two children with FLT3-ITD-positive AML who received long-term treatment with sorafenib. The first patient was a 10-year-old boy treated with 2 courses on the RELHEM protocol. The N-oxide metabolite ratio on day 7 was 0.44 (Figure 4). While waiting for hematopoietic stem cell transplantation (HSCT), he developed RSV infection and then received single-agent sorafenib 200 mg once daily for

approximately 8 months. During this time, the N-oxide metabolite ratio on day 103 was 0.43. Shortly thereafter, antifungal prophylaxis with oral voriconazole 150 mg twice daily was started. With persistent marrow infiltration with leukemic cells, the sorafenib dose was increased to 200 mg twice daily on day 321. On days 338 and 383, N-oxide metabolite ratio was dramatically reduced to 0.06 and 0.05, respectively, compared to previous values without concurrent voriconazole. The second patient was a 10-year-old boy treated with 1 course of sorafenib 200 mg/m^2 after Induction II on the AML08 protocol. On day 15, the N-oxide metabolite ratio was 0.29. He received a HSCT and relapsed 15 months later. On day 554, sorafenib 200 mg once daily was initiated with concurrent oral voriconazole 150 mg twice daily. On days 575 and 607, the N-oxide metabolite ratio was dramatically reduced to 0.05 and 0.09, respectively, when compared to previous values in the absence of voriconazole (Figure 4). Consistent with the *in vitro* data, sorafenib N-oxide metabolite ratio was greatly reduced upon cotreatment with posaconazole and voriconazole.

Sorafenib Metabolism in Human Liver Samples

The effects of age and sex on sorafenib CYP and UGT-mediated metabolism were studied in microsomes (HLM) isolated from 52 human liver samples. CYP-mediated metabolism to sorafenib N-oxide as a function of age and sex is illustrated in Figure 5A. A non-significant trend for increased sorafenib N-oxide formation was observed in males compared to females in the 10 to 15 year age group (median, −1.1 v*ersus* −1.5 log[μM/min/mg HLM]) (Figure 5B). Analysis of sorafenib glucuronidation demonstrated no notable trends for either age or sex (Supplemental Figures 5A and 5B).

To determine whether CYP-mediated sorafenib metabolism corresponded with enzyme mRNA expression, we used quantitative PCR analysis to measure liver CYP3A4 mRNA expression. Similar to sorafenib N-oxide production, a non-significant trend for increased CYP3A4 expression was observed in males compared to females in the 10 to 15 year age group (median, 16.8 *versus* 13.0 $\log_2$[transcript/ng RNA]) (Figures 5C and 5D). CYP3A4 mRNA expression was correlated with sorafenib N-oxide production (r^2 - 0.33, $p = 0.0001$), suggesting that the variability observed in sorafenib N-oxide formation in liver samples was partially due to variability in CYP3A4 expression. In contrast, UGT1A9 mRNA expression displayed no trends with regard to age and sex and did not correlate with the level of sorafenib glucuronidation (Supplemental Figures 5C-E).

Discussion

In this study, we describe a comprehensive characterization of sorafenib metabolism *in vitro* and *in vivo* in children with AML. Of a panel of CYP and UGT enzymes evaluated, we demonstrated that sorafenib is almost exclusively metabolized to sorafenib N-oxide by CYP3A4 and to sorafenib glucuronide by UGT1A9. Although no age-related differences in sorafenib steady-state apparent oral clearance were seen, we observed a higher rate of sorafenib conversion to the active metabolite sorafenib N-oxide in children compared to that reported previously in adults with cancer (6, 7). To our knowledge, we report the first analysis of sorafenib glucuronidation in cancer patients. On average, sorafenib glucuronide and N-oxide metabolite ratios were similar (~ 0.30). We showed *in vitro* that the clinically useful azole antifungals posaconazole and voriconazole potently inhibited sorafenib metabolism to sorafenib N-oxide, but were weak inhibitors of sorafenib glucuronidation. A drug-drug interaction was demonstrated *in vivo*, where both posaconazole and voriconazole reduced N-oxide production to negligible levels.

The majority of kinase inhibitors that are approved for the treatment of cancer are primarily metabolized by CYP3A4 to an active metabolite (10, 24, 25, 26). In general, active metabolites of kinase inhibitors represent approximately 10% or less of exposure to parent

drug. One exception is sunitinib, where the active metabolite N-desethyl-sunitinib accounts for 30–50% of total pharmacologic activity in cancer patients (11, 27, 28). Here, we demonstrate that sorafenib provides another exception to the other kinase inhibitors in that we observed a mean 27% conversion to sorafenib N-oxide in children ranging in age from 1 to 19 years, and even higher conversion (40%) in boys ≤ 10 years. In view of the circulating concentrations of sorafenib N-oxide in children (mean ~ 2 to 3 μM at sorafenib 200 mg/m^2), it is believed to contribute significantly to sorafenib-induced antitumor activity.

The maturation of drug-metabolizing enzymes during childhood development is considered one of the main factors accounting for age-associated changes in drug metabolism and has been extensively studied (12). *In vitro*, CYP3A activity is low before birth, increases rapidly after birth, and reaches a peak in infants to levels slightly higher than those in adults (12, 13). However, *in vivo* evaluations of CYP3A4 activity have yielded inconsistent results. For example, one study showed no differences in CYP3A activity among older infants, children and adults (14), whereas another study demonstrated that CYP3A4 activity was lower in infants and children up to 2 years but higher in older children 3 to 13 years when compared to adults (15).

To gain further insight into age-associated changes in sorafenib N-oxide formation, we evaluated CYP3A4 gene expression and sorafenib metabolism in a large cohort of human liver samples from children < 20 years old. We observed substantial variability in metabolism to sorafenib N-oxide across all age groups, and the same trend for higher conversion in boys. However, peak N-oxide conversion was observed between the ages of 10 and 15 years *in vitro* instead of 6 to 10 years in our patient population. However, both our *in vitro* and *in vivo* findings are in line with those from a separate cohort of liver samples, where a trend for higher CYP3A4-mediated testosterone and midazolam metabolism was observed in males versus females <10 years as well as in a group aged 10 to 19 years (16). We also showed that CYP3A4 mRNA expression was correlated with sorafenib N-oxide formation. Thus, differential activity of nuclear receptors and/or other proteins known to regulate CYP3A4 transcription, such as PXR (17), CAR (18), and HNF4α (19), could explain the inter-patient differences in sorafenib N-oxidation in the liver samples. Discrepancies in peak occurrence of sorafenib N-oxide formation between our patient population and liver samples could also be due to differences in the timing of pubertal maturation. It is known that changes in growth hormone and sex steroids that occur during adolescence can affect the expression of drug metabolizing enzymes (20, 29). The observed enhanced N-oxide formation in boys compared to girls may suggest a preferential effect of androgens on sorafenib metabolism, as has been described previously for carbamazepine epoxidation by CYP3A4 (21). Ultimately there are limitations to evaluating drug metabolizing enzyme expression and activity in frozen human liver samples such as the lack of adequate documentation of concurrent medications and comorbidities of the donor, although an attempt was made to document these factors in the liver population tested.

Less is known regarding developmental changes in UGT1A9. Analysis of livers from 16 pediatric patients aged 6 to 24 months showed that UGT1A9 mRNA expression was lower in infants compare to adult livers > 25 years of age (22). Although no obvious age-related trends in sorafenib glucuronidation were observed in our pediatric population or liver samples, glucuronidation rates, as well as sorafenib N-oxide formation, appeared the most variable in younger children (Figure 2C). The latter observation suggests that developmental or maturational changes in drug metabolizing enzymes likely affect sorafenib metabolism.

A drug-drug interaction between azole antifungals and sorafenib was demonstrated both *in vitro* and *in vivo*. In several cases of children receiving concurrent posaconazole or voriconazole with sorafenib, we observed significantly reduced conversion of sorafenib to

sorafenib N-oxide. Since sorafenib doses were changing throughout the clinical time course, we could not determine if sorafenib exposure was altered by co-treatment with azoles in these particular cases. In healthy subjects, ketoconazole inhibited sorafenib metabolism to the N-oxide, but it had no effect on sorafenib plasma clearance (3). Therefore, posaconazole and voriconazole are not expected to significantly alter sorafenib exposure. In light of the potential contribution of sorafenib N-oxide to antitumor activity and the ability of azoles antifungals to inhibit N-oxide production *in vivo*, the use of alternative antifungal agents should be considered with sorafenib therapy unless azole antifungals are medically indicated.

In conclusion, we have identified several factors affecting inter-patient variability in sorafenib metabolism to its active metabolite sorafenib N-oxide including age, sex, and concurrent treatment with azole antifungals. Since the active metabolite is likely to contribute to antitumor activity, this knowledge may provide important considerations for the effective use of sorafenib in childhood AML and possibly other pediatric cancers. The effect of ontogeny on CYP3A4-mediated metabolism may also be relevant to the clinical use of other kinase inhibitors.

Supplementary Material

Refer to Web version on PubMed Central for supplementary material.

Acknowledgments

Supported by Grants No. CA138744, CA021765, and CA023944 from the National Cancer Institute, NIH/NIGMS Grant R01 GM094418, and by the American Lebanese Syrian Associated Charities.

References

1. Fabian MA, Biggs WH 3rd, Treiber DK, Atteridge CE, Azimioara MD, Benedetti MG, et al. A small molecule-kinase interaction map for clinical kinase inhibitors. Nat Biotechnol. 2005; 23:329–336. [PubMed: 15711537]
2. Mori S, Cortes J, Kantarjian H, Zhang W, Andreef M, Ravandi F. Potential role of sorafenib in the treatment of acute myeloid leukemia. Leuk Lymphoma. 2008; 49:2246–2255. [PubMed: 19052971]
3. Lathia C, Lettieri J, Cihon F, Gallentine M, Radtke M, Sundaresan P. Lack of effect of ketoconazole-mediated CYP3A inhibition on sorafenib clinical pharmacokinetics. Cancer Chemother Pharmacol. 2006; 57:685–692. [PubMed: 16133532]
4. Peer CJ, Sissung TM, Kim A, Jain L, Woo S, Gardner ER, et al. Sorafenib Is an Inhibitor of UGT1A1 but Is Metabolized by UGT1A9: Implications of Genetic Variants on Pharmacokinetics and Hyperbilirubinemia. Clin Cancer Res. 2012; 18:2099–2107. [PubMed: 22307138]
5. Minami H, Kawada K, Ebi H, Kitagawa K, Kim YI, Araki K, et al. Phase I and pharmacokinetic study of sorafenib, an oral multikinase inhibitor, in Japanese patients with advanced refractory solid tumors. Cancer Sci. 2008; 99:1492–1498. [PubMed: 18477034]
6. Inaba H, Rubnitz JE, Coustan-Smith E, Li L, Furmanski BD, Mascara GP, et al. Phase I pharmacokinetic and pharmacodynamic study of the multikinase inhibitor sorafenib in combination with clofarabine and cytarabine in pediatric relapsed/refractory leukemia. J Clin Oncol. 2011; 29:3293–3300. [PubMed: 21768474]
7. Pratz KW, Cho E, Levis MJ, Karp JE, Gore SD, McDevitt M, et al. A pharmacodynamic study of sorafenib in patients with relapsed and refractory acute leukemias. Leukemia. 2010; 24:1437–1444. [PubMed: 20535150]
8. Irizarry RA, Bolstad BM, Collin F, Cope LM, Hobbs B, Speed TP. Summaries of Affymetrix GeneChip probe level data. Nucleic Acids Res. 2003; 31:e15. [PubMed: 12582260]

9. Saad AH, DePestel DD, Carver PL. Factors influencing the magnitude and clinical significance of drug interactions between azole antifungals and select immunosuppressants. Pharmacotherapy. 2006; 26:1730–1744. [PubMed: 17125435]
10. Castellino S, O'Mara M, Koch K, Borts DJ, Bowers GD, MacLauchlin C. Human metabolism of lapatinib, a dual kinase inhibitor: implications for hepatotoxicity. Drug Metab Dispos. 2012; 40:139–150. [PubMed: 21965624]
11. Britten CD, Kabbinavar F, Hecht JR, Bello CL, Li J, Baum C, et al. A phase I and pharmacokinetic study of sunitinib administered daily for 2 weeks, followed by a 1-week off period. Cancer Chemother Pharmacol. 2008; 61:515–524. [PubMed: 17505827]
12. de Wildt SN, Kearns GL, Leeder JS, van den Anker JN. Cytochrome P450 3A: ontogeny and drug disposition. Clin Pharmacokinet. 1999; 37:485–505. [PubMed: 10628899]
13. Lacroix D, Sonnier M, Moncion A, Cheron G, Cresteil T. Expression of CYP3A in the human liver--evidence that the shift between CYP3A7 and CYP3A4 occurs immediately after birth. Eur J Biochem. 1997; 247:625–634. [PubMed: 9266706]
14. Dundee JW, Halliday NJ, Harper KW, Brogden RN. Midazolam. A review of its pharmacological properties and therapeutic use. Drugs. 1984; 28:519–543. [PubMed: 6394264]
15. Hughes J, Gill AM, Mulhearn H, Powell E, Choonara I. Steady-state plasma concentrations of midazolam in critically ill infants and children. Ann Pharmacother. 1996; 30:27–30. [PubMed: 8773161]
16. Yang X, Zhang B, Molony C, Chudin E, Hao K, Zhu J, et al. Systematic genetic and genomic analysis of cytochrome P450 enzyme activities in human liver. Genome Res. 2010; 20:1020–1036. [PubMed: 20538623]
17. Bertilsson G, Heidrich J, Svensson K, Asman M, Jendeberg L, Sydow-Backman M, et al. Identification of a human nuclear receptor defines a new signaling pathway for CYP3A induction. Proc Natl Acad Sci U S A. 1998; 95:12208–12213. [PubMed: 9770465]
18. Goodwin B, Hodgson E, D'Costa DJ, Robertson GR, Liddle C. Transcriptional regulation of the human CYP3A4 gene by the constitutive androstane receptor. Mol Pharmacol. 2002; 62:359–365. [PubMed: 12130689]
19. Tirona RG, Lee W, Leake BF, Lan LB, Cline CB, Lamba V, et al. The orphan nuclear receptor HNF4alpha determines PXR- and CAR-mediated xenobiotic induction of CYP3A4. Nat Med. 2003; 9:220–224. [PubMed: 12514743]
20. Kennedy M. Hormonal regulation of hepatic drug-metabolizing enzyme activity during adolescence. Clin Pharmacol Ther. 2008; 84:662–673. [PubMed: 18971926]
21. Nakamura H, Torimoto N, Ishii I, Ariyoshi N, Nakasa H, Ohmori S, et al. CYP3A4 and CYP3A7-mediated carbamazepine 10,11-epoxidation are activated by differential endogenous steroids. Drug Metab Dispos. 2003; 31:432–438. [PubMed: 12642469]
22. Strassburg CP, Strassburg A, Kneip S, Barut A, Tukey RH, Rodeck B, et al. Developmental aspects of human hepatic drug glucuronidation in young children and adults. Gut. 2002; 50:259–265. [PubMed: 11788570]
23. Yong WP, Ramirez J, Innocenti F, Ratain MJ. Effects of ketoconazole on glucuronidation by UDP-glucuronosyltransferase enzymes. Clin Cancer Res. 2005; 11:6699–6704. [PubMed: 16166450]
24. Di Gion P, Kanefendt F, Lindauer A, Scheffler M, Doroshyenko O, Fuhr U, et al. Clinical pharmacokinetics of tyrosine kinase inhibitors: focus on pyrimidines, pyridines and pyrroles. Clin Pharmacokinet. 2011; 50:551–603. [PubMed: 21827214]
25. Ling J, Johnson KA, Miao Z, Rakhit A, Pantze MP, Hamilton M, et al. Metabolism and excretion of erlotinib, a small molecule inhibitor of epidermal growth factor receptor tyrosine kinase, in healthy male volunteers. Drug Metab Dispos. 2006; 34:420–426. [PubMed: 16381666]
26. Speed B, Bu HZ, Pool WF, Peng GW, Wu EY, Patyna S, et al. Pharmacokinetics, distribution, and metabolism of [14C]sunitinib in rats, monkeys, and humans. Drug Metab Dispos. 2012; 40:539–555. [PubMed: 22180047]
27. Dubois SG, Shusterman S, Ingle AM, Ahern CH, Reid JM, Wu B, et al. Phase I and pharmacokinetic study of sunitinib in pediatric patients with refractory solid tumors: a children's oncology group study. Clin Cancer Res. 2011; 17:5113–5122. [PubMed: 21690570]

28. Faivre S, Delbaldo C, Vera K, Robert C, Lozahic S, Lassau N, et al. Safety, pharmacokinetic, and antitumor activity of SU11248, a novel oral multitarget tyrosine kinase inhibitor, in patients with cancer. J Clin Oncol. 2006; 24:25–35. [PubMed: 16314617]

29. Veal GJ, Hartford CM, Stewart CF. Clinical pharmacology in the adolescent oncology patient. J Clin Oncol. 2010; 28:4790–4799. [PubMed: 20439647]

Statement of Translational Relevance

Sorafenib is a multi-kinase inhibitor being evaluated in children with acute myeloid leukemia (AML) and solid tumors. We investigated the role of ontogeny in sorafenib metabolism to the equipotent active metabolite sorafenib N-oxide in thirty children with AML. No age-related differences in sorafenib clearance were observed, but a higher rate of sorafenib conversion to the N-oxide was seen in children compared to that reported previously in adults, with highest conversion in boys. A similar trend was observed in 52 human liver samples. In a panel of purified human cytochrome P450 (CYP) enzymes, sorafenib was exclusively metabolized by CYP3A4. The azoles posaconazole and voriconazole potently inhibited sorafenib N-oxide formation *in vitro* and *in vivo* in 3 children with AML. Several factors affecting inter-patient variability in sorafenib metabolism were identified including age, sex, and concurrent treatment with azoles, which may be relevant to the clinical use of sorafenib in children.

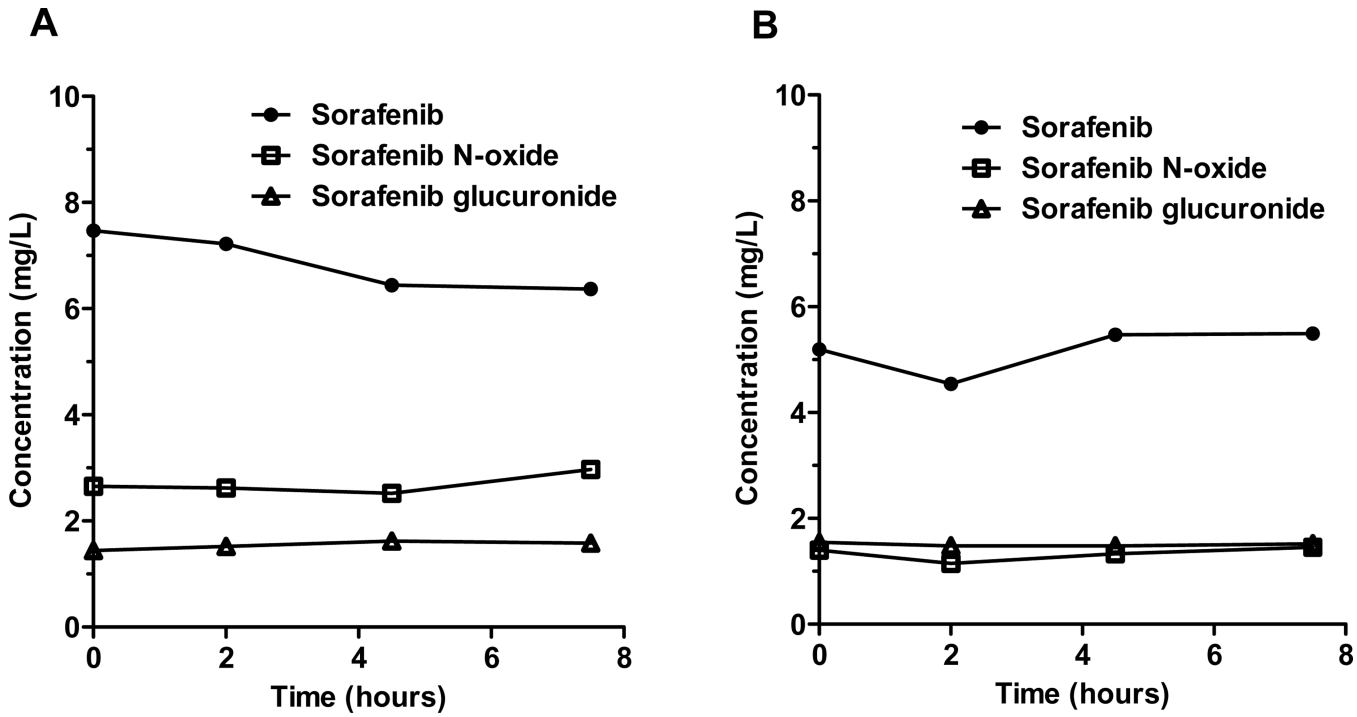

Figure 1.
Mean steady-state sorafenib, sorafenib N-oxide, and sorafenib glucuronide concentrations at sorafenib doses of (**A**) 150 mg/m^2 and (**B**) 200 mg/m^2.

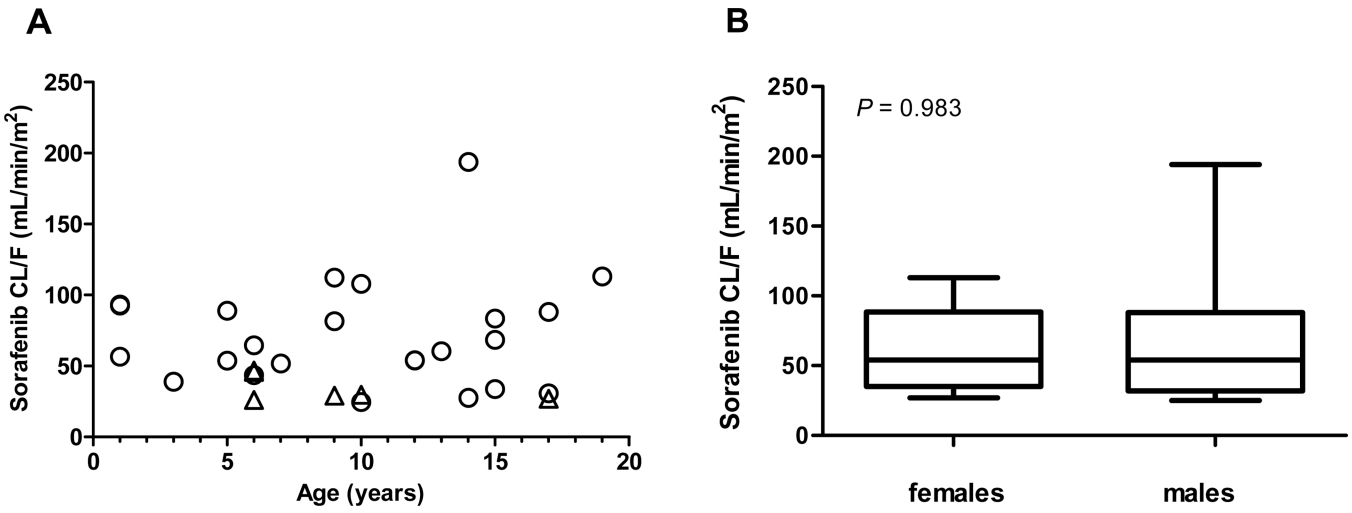

Figure 2.

Steady-state sorafenib apparent oral clearance (CL/F) as a function of age and sex. (**A**) Sorafenib CL/F at 200 mg/m^2 (circles) and 150 mg/m^2 (triangles) according to age. (**B**) Box plot of values for sorafenib CL/F according to sex. *P* values are from a Wilcoxon rank-sum test.

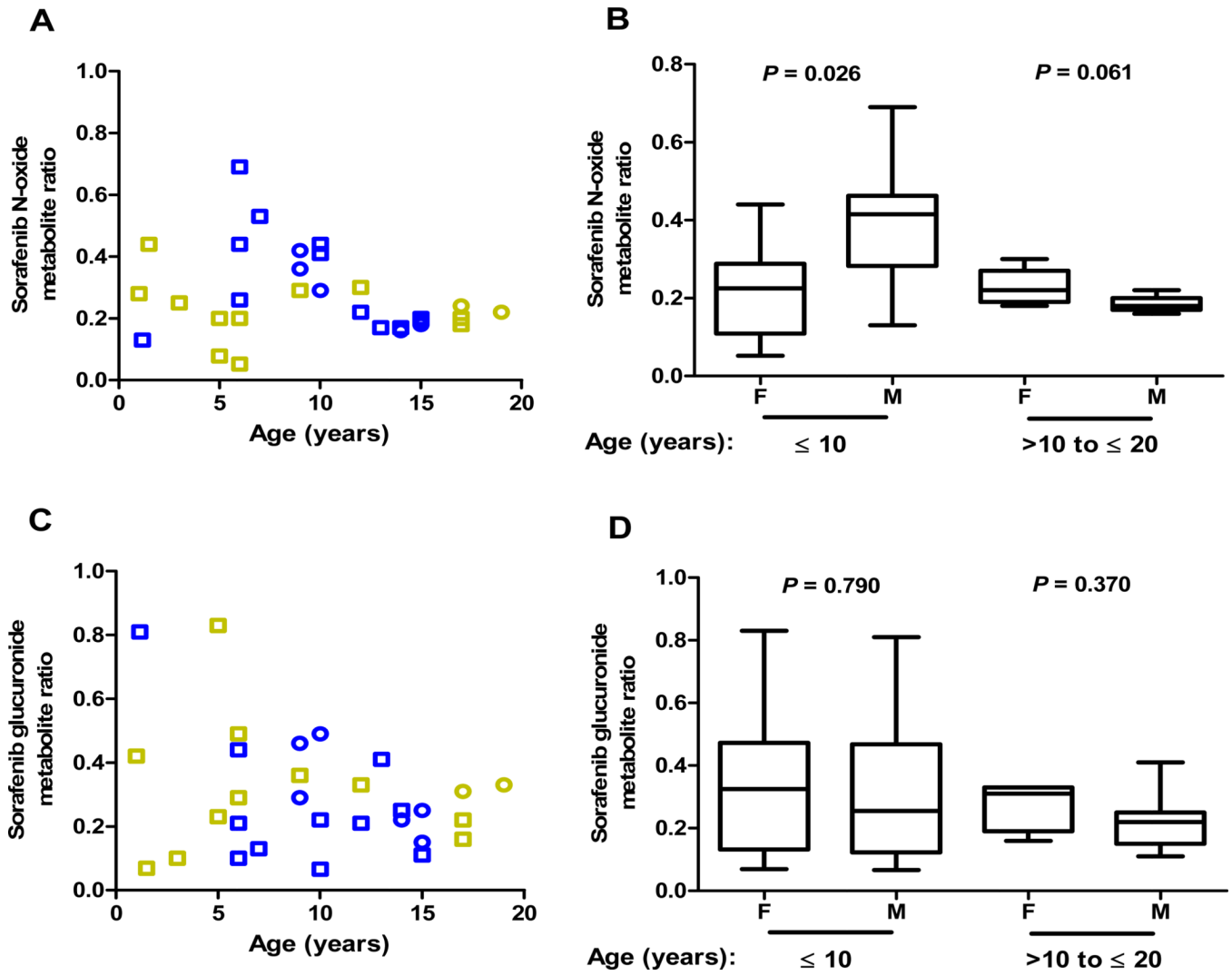

Figure 3. Age- and sex-dependent sorafenib metabolism

(**A**) Sorafenib N-oxide metabolite ratio at steady-state as a function of age and sex. Circles: newly-diagnosed AML; squares: refractory/relapsed AML; blue symbols: males; gold symbols: females. (**B**) Box plot of values for sorafenib N-oxide metabolite ratio according to sex and age groups. *P* values are from a Wilcoxon rank-sum test. (**C**) Sorafenib glucuronide metabolite ratio at steady-state as a function of age and sex. Circles: newly-diagnosed AML; squares: refractory/relapsed AML; blue symbols: males; gold symbols: females. (**D**) Box plot of values for sorafenib glucuronide metabolite ratio according to sex and age groups. *P* values are from a Wilcoxon rank-sum test.

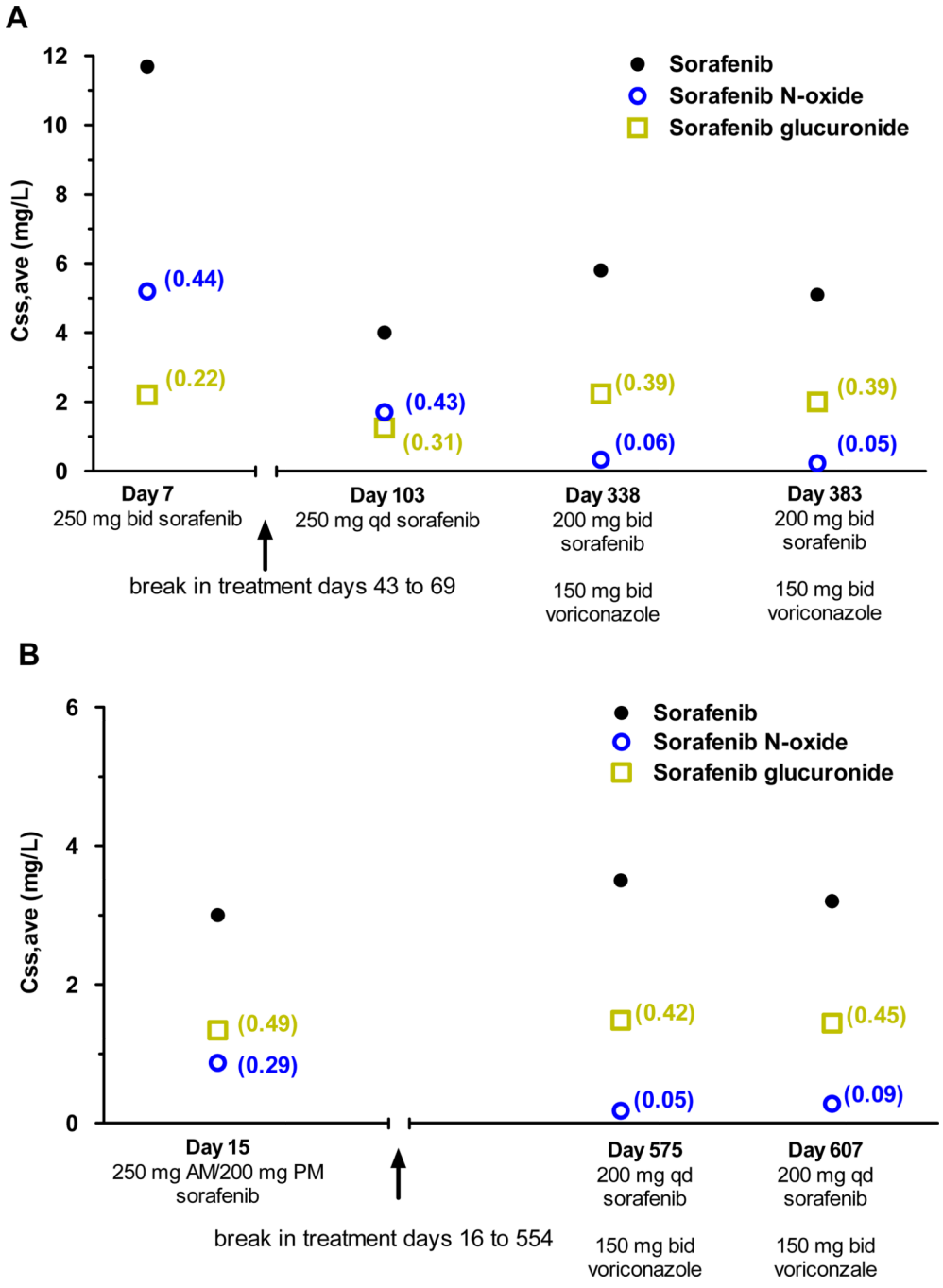

Figure 4. Effect of voriconazole treatment on sorafenib metabolism in 2 children with FLT3-ITD-positive AML

Average steady-state plasma concentrations (Css,ave) are shown for sorafenib, sorafenib N-oxide, and sorafenib glucuronide as a function of time. Values for sorafenib metabolite ratio and sorafenib glucuronide metabolite ratio are shown in the parentheses next to the observed concentration.

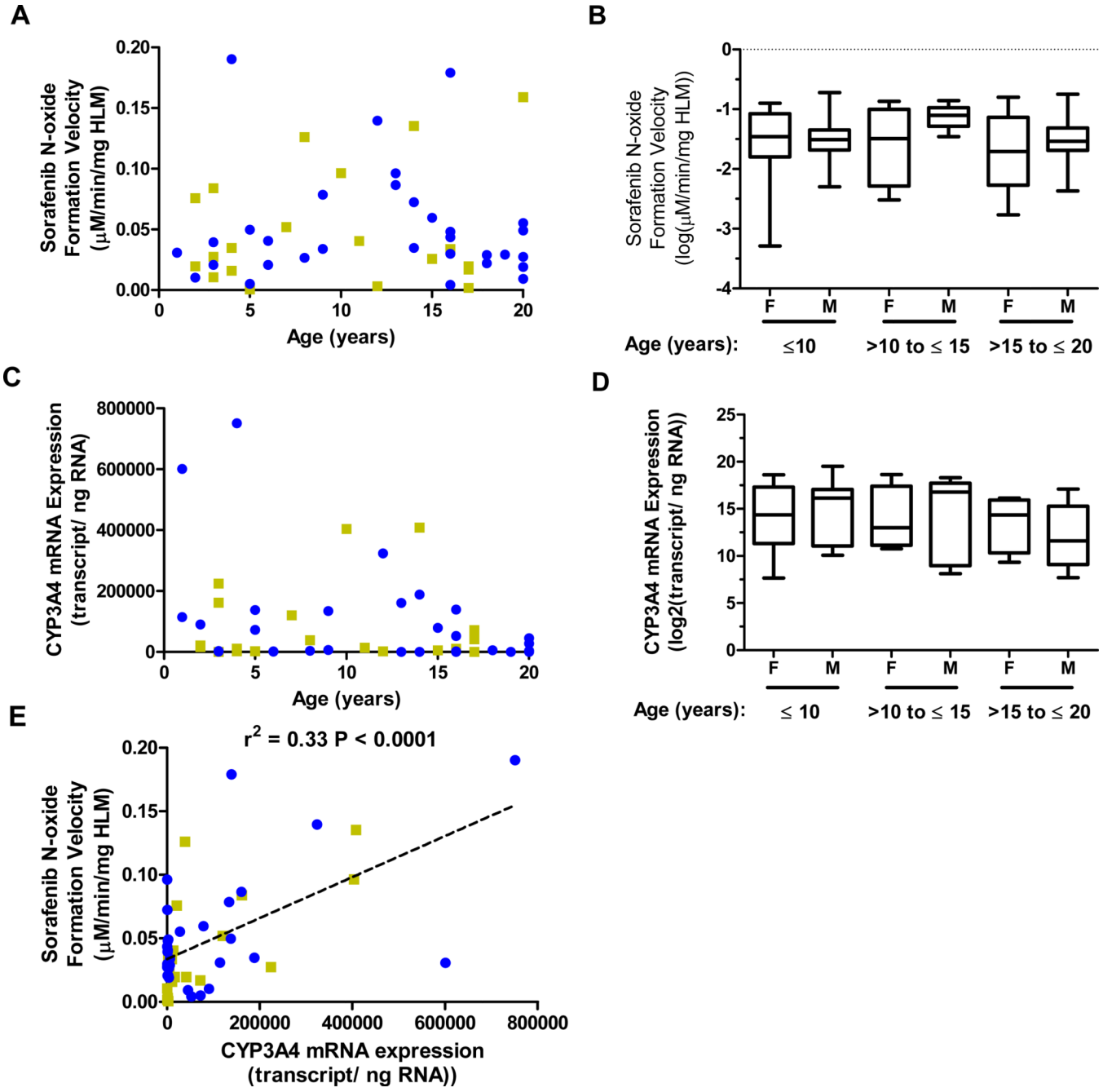

Figure 5. Age- and sex-dependent sorafenib N-oxide formation and correlation with CYP3A4 mRNA expression in human liver samples

(**A**) Sorafenib N-oxide formation velocity as a function of age and sex. *In vitro* CYP-mediated metabolic reactions were performed in microsomes isolated from human liver samples using sorafenib 10 µM and an incubation time of 60 min. Data represent the mean formation velocity from triplicate reactions. Blue symbols: males; gold symbols: females. (**B**) Box plot of sorafenib N-oxide velocity values according to sex and age groups. (**C**) CYP3A4 mRNA expression as a function of age and sex. Quantitative PCR was performed on RNA isolated from human liver samples. Data represent the mean mRNA expression from 2 independent experiments performed with triplicate measurements. Blue circles:

males; gold squares: females. (**D**) Box plot of CYP3A4 mRNA expression according to sex and age groups. (**E**) CYP3A4 mRNA expression plotted as a function of sorafenib N-oxide velocity. The line, r^2 values, and *P* values are from linear regression analysis. Blue circles: males; gold squares: females.